16

Ikeda Mapping Dynamics

The Ikeda map I we study is given by

$$I : z \mapsto R + C_2 z \exp(i(C_1 - C_3/(1 + |z|^2)), \quad z \in C, \tag{16.1}$$

where C is the complex plane of the variable $z = x + iy$ and R, $C1$, $C2$, and $C3$ are real constants (mapping parameters). The Ikeda map occurs in the modeling of optical recording media (crystals) [60]. The numerical results obtained to date (see [94], [120], [48], [37], [144]) show that under certain parameter values the Ikeda map exhibits highly complicated dynamical behavior. In particular, the Ikeda map can have infinitely many hyperbolic periodic orbits, which are located in a bounded part of C, and a strange attractor (the Ikeda attractor). We also consider the modifications of the Ikeda map like mappings reversing orientation and hyperbolic. The aim of the chapter is to give an analysis of the topological structure of orbits by symbolic dynamics methods (the package ASIDS) and by iterations of curves (the package Line). We also present an analysis of orbit behavior near fixed and periodic points and of bifurcations that lead to chaotic attractors as parameters vary.

16.1 Analytical Results

In this section we give some simple analytical results on the Ikeda map we need in the sequel. In the real notation the Ikeda map takes the form

$$I : (x, y) \mapsto (R + C_2(x\ \cos\tau - y\ \sin\tau), C_2(x\ \sin\tau + y\ \cos\tau)), \tag{16.2}$$

where $\tau = C_1 - C_3/(1 + x^2 + y^2)$. Some obvious properties of the Ikeda map are listed below.

1. The map I can be viewed as a composition of the three diffeomorphisms T_1, T_2, and T_3 of the plane onto itself:

$$I = T_3 \circ T_2 \circ T_1,$$

where $T_1(x,y) = (x\cos\tau - y\sin\tau, x\sin\tau + y\cos\tau)$ is a rotation through the angle $\tau = \tau(r), r^2 = x^2 + y^2$, $T_2(u,v) = (C_2u, C_2v)$ is a linear homothetic, and $T_3(s,t) = (R+s,t)$ is a translation along the real axis.

2. If $C_2 > 0$ then I is an orientation preserving diffeomorphism of the plane onto itself.
3. If $|C2| < 1$ then the map I is dissipative, i.e. there exists an $h > 0$ such that
$$\lim_{n\to\infty} \sup ||I^n(x,y)|| < h$$
for each point (x,y).
4. If $|C_2| < 1$ then every disk $K_r = \{(x,y) : x^2 + y^2 < r^2\}$ with the radius $r > |R|/(1-|C2|)$ is mapped into itself, i.e. $I(K_r) \subset int\, K_r$.
5. For every point (x,y) the Jacobian of I is of the form $\det DI(x,y) = {C_2}^2$. Thus, if $|C_2| < 1$ then I contracts the area, i.e. for the Lebesque measure of every bounded measurable set U we have
$$mes\, I(U) \leq mes\, U.$$

Let $|C_2| < 1$. The properties listed above imply the following:

1. Every bounded invariant set $U (I(U) = U)$ is contained in the disk $K(r^*)$ with the radius $r^* = |R|/(1-|C_2|)$. Let A_g be the maximal bounded invariant set of I contained in $K(r^*)$:
$$A_g = \bigcap_{n=0}^{\infty} I^n(K(r^*)).$$
It is well known that the set A_g is closed connected and asymptotically stable in the large, i.e. A_g is a global attractor. By 5, A_g has measure zero: $mes\, A_g = 0$.
2. The behavior of orbits of I is entirely determined by the behavior of orbits from A_g. In particular, periodic, nonwandering, and chainrecurrent orbits of I are contained in A_g. Results of numerical explorations mentioned above indicate that under certain parameter values the diffeomorphism I can have infinitely many hyperbolic periodic orbits with periods tending to infinity. This leads to the existence of homoclinic orbits and indecomposable continua in A_g. The last means that A_g has a very intricate topological structure.

16.2 Numerical Results

Numerical simulations of the dynamical behavior of the map I have been carried out with $C_1 = 0.4$, $C_2 = 0.9$, $C_3 = 6.0$. The parameter R takes the values within the segment $[0; 1.1]$ increasing by $R = 0.01$. For each value of R, phase portraits are indexed by small letters a, b, anew. The obtained

values will be given in approximations. Results of the numerical study are the following.

As R increases from 0 to approximately 0.367, the global attractor A_g is a single asymptotically stable fixed point, i.e. I offers the convergence property.

16.2.1 $R = 0.3$

The Ikeda map has the fixed point $A_0(0.1766, 0.2298)$. This fixed point attracts all other orbits.

16.2.2 $R = 0.4$

The Ikeda map has three fixed points: the fixed point $A_0(0.2280, 0.2568)$, the hyperbolic saddle point $H_0(3.0508, -1.6442)$, and the stable focus $S_0(3.7763, 0.8930)$, see Fig. 16.1,a where the global attractor of the map is shown. The unstable manifold $W^u(H_0)$ of H_0 consists of two separatrices; the limit set of the left separatrix is the sink ${A_0}^* = A_0$ and the limit set of the right one is S_0. However, while S_0 is a regular focus, the sink ${A_0}^*$ has a sufficiently complicated topological structure (see Fig. 16.1,b). The stable manifold $W^s(H_0)$ of the saddle H_0 separates the basins $W^s({A_0}^*)$ and $W^s(S_0)$ of the attractors ${A_0}^*$ and S_0.

16.2.3 $R = 0.5$

While R increases from $R = 0.4$ to $R = 0.5$ the sink A_0^* bifurcates to the attractor A which when $R = 0.5$ contains the sink $A_0(0.2784, 0.2734)$, the period

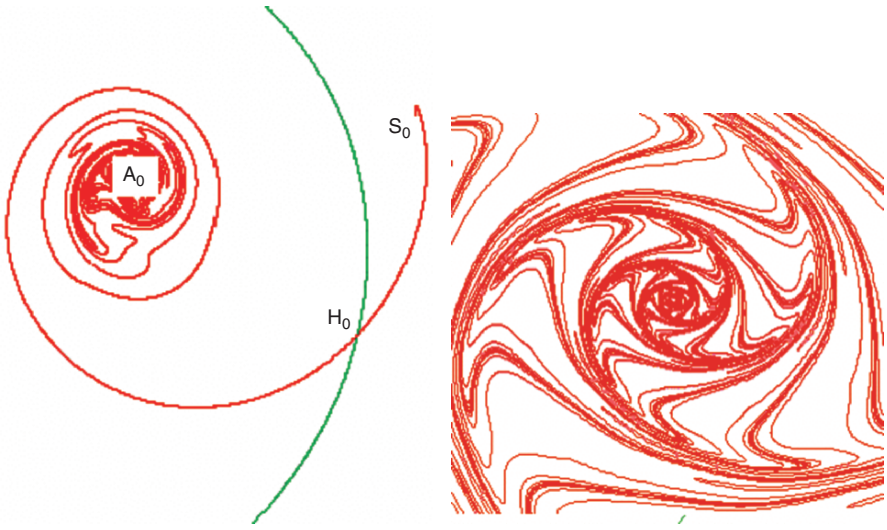

Fig. 16.1. Ikeda map for $R = 0.4$

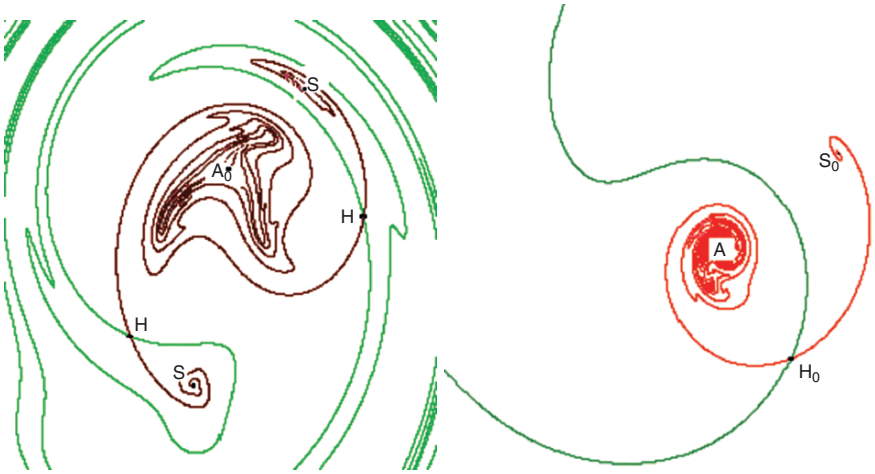

Fig. 16.2. Ikeda map for $R = 0.5$

2 sink $S(0.0897, -0.7195), (0.6758, 0.6141)$, and the period 2 hyperbolic saddle $H(1.0017, 0.0376), (-0.2517, -0.4987)$ (see Fig. 16.2,a). The unstable separatrices $W^u(H)$ of H ends at A_0 and S. The closure of the unstable manifold $W^u(H)$ (colored dark) coincides with the attractor $A = W^u(H) + A_0 + S$. The stable manifold $W^s(H)$ (colored light) separates the basins of attraction of A_0 and S. The basin boundary of A is formed by the stable manifold $W^s(H_0)$ of the hyperbolic fixed point H_0 at approximately $(2.2330, -2.3346)$ (see Fig. 16.2,b). The unstable manifold $W^u(H_0)$ of H_0 consists of two separatrices, the left one ends at A and the right one ends at the sink $S_0(3.5231, 2.1942)$. The closure of $W^u(H_0)$ is the global attractor $A_g = W^u(H_0) + A + S_0$ of the map. This form of the global attractor is preserved up to the parameter value $R = 1$, except that the structure of the attractor A varies over a wide range.

16.2.4 $R = 0.6$

The sink $A_0(0.3397, 0.2809)$, the period 2 hyperbolic orbit $H(1.0094, -0.1100)$, $(-0.2110, -0.4211)$, and the period 2 sink $S(0.5997, 0.6757), (0.2188, -0.7184)$ are contained in the attractor A. The unstable manifold $W^u(H)$ of each point of the orbit H is formed by two separatrices, one of these separatrices ends at the sink A_0, (see Fig. 16.3,a), while the other one intersects the stable manifold $W^s(H)$, giving rise to a sequence of homoclinic points. Some homoclinic points are listed in the following list:

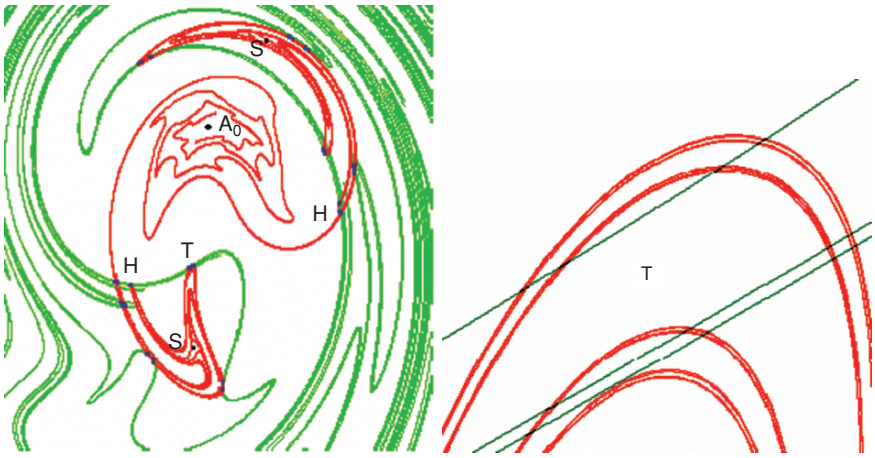

a b

Fig. 16.3. Ikeda map for $R = 0.6$

$(x = 0.192905, y = -0.358028); (x = -0.208911, y = -0.421623);$
$(x = 0.193456, y = -0.357745); (x = -0.210681, y = -0.421222);$
$(x = -0.196432, y = -0.424266); (x = -0.210709, y = -0.421216);$
$(x = -0.197692, y = -0.420132); (x = -0.210990, y = -0.421152);$
$(x = -0.211047, y = -0.421139); (x = -0.210997, y = -0.421150);$
$(x = -0.208703, y = -0.421670); (x = -0.211034, y = -0.421142).$

The Figure 16.3,b where the stable $W^s(H)$ and unstable $W^u(H)$ manifolds are depicted, indicates the transverse character of intersections of these manifolds near T. Since at $R = 0.5$ the manifolds $W^u(H)$ and $W^s(H)$ are disjoint then there exists a parameter value $R^*, 0.5 < R^* < 0.6$, such that the manifold $W^u(H)$ is tangent to the manifold $W^s(H)$. The stable manifold $W^s(H)$ of the orbit H forms the boundary of the basins of attraction of the sink A_0 and the period 2 attractor A_2, which contains the period 2 sink S. In Fig. 16.4,c is shown the basin of attraction of A_2 (colored white grey). Its component containing the point $(0.2188, -0.7184)$ of the sink S is shown in Fig. 16.4,d.

The attractor A_2 is a closure of the unstable manifold $W^u(P)$ of the period 6 hyperbolic orbit $P(0.1869, -0.5785)$, $(0.3556, 0.7053)$, $(0.2818, -0.7800)$, $(0.6249, 0.6969)$, $(0.1343, -0.7635)$, $(0.8751, 0.4730)$. Each connected component of $W^u(P)$ consists of two separatrices, the one ends at the sink S, while the other one ends at the chaotic attractor A_3 (see Fig. 16.4,e). A_3 contains the attractor A_4, induced by the unstable manifold $W^u(Q)$ of the period 6 orbit Q. In Fig. 16.4,f are shown the point $(0.2056, -0.4874)$ of the orbit Q (depicted as a black dot) and its stable and unstable manifolds. The attractor A_4 is a

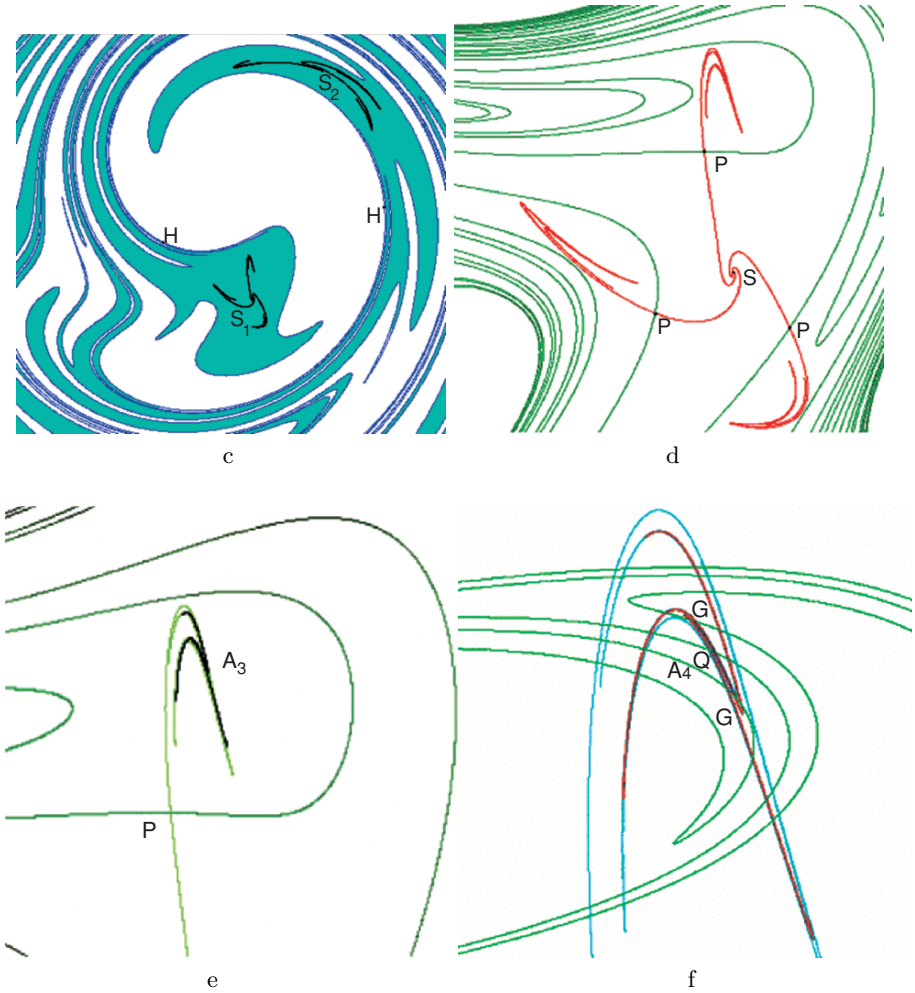

Fig. 16.4. Ikeda map for $R = 0.6$

closure of the unstable manifold $W^u(Q)$, which ends at the period 12 sink G. Fig. 16.4,f presents also two points $(0.2022, -0.4816)$ and $(0.2095, 0.4953)$ of the orbit G.

It is interesting to note that the stable and unstable manifolds are tangent at Q forming a sink. The global attractor A is a closure of the unstable manifold of the orbit H : $A = W^u(H) + A_2 + A_0$. The stable manifold $W^s(H_0)$ of the hyperbolic point $H_0(1.7660, -2.4891)$ is the common boundary of basins of attraction of A and the sink $S_0(3.3064, 2.8382)$. The displacement of A, H_0 and S_0 is similar to that in the cases $R = 0.5$ and $R = 0.7$.

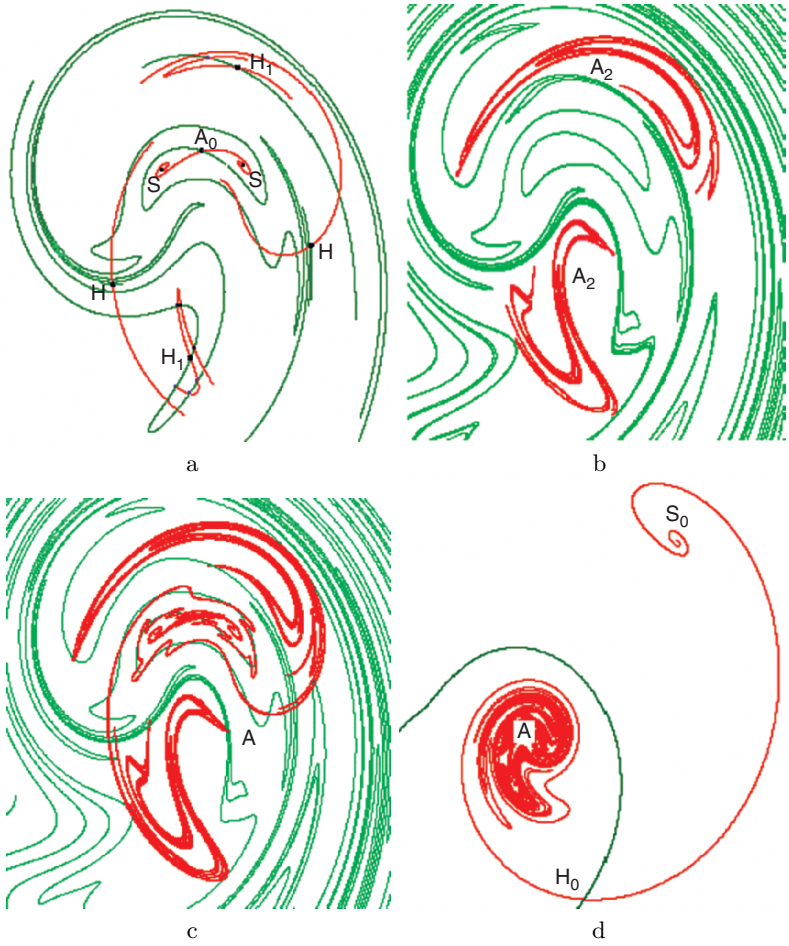

Fig. 16.5. Ikeda map for $R = 0.7$

16.2.5 $R = 0.7$

The Ikeda map with $R = 0.7$ has the inverse saddle fix point $A_0(0.3804, 02817)$ (see Fig. 16.5,a). The unstable manifold $W^u(A_0)$ of A_0 ends at the sink formed by a pair of the period 2 points $S(0.1548, 0.2030)$, $(0.6110, 0.2118)$ which is a minimal attractor. The inverse saddle point A_0 and the period 2 sink S arise from the sink A_0 while R varies from $R = 0.6$ up to $R = 0.7$. A closure of the unstable manifold $W^u(A_0)$ forms the attractor $A_1 = W^u(A_0) + S$. The Ikeda map reverse the orientation of $W^u(A_0)$ and hence the orientation of $W^s(A_0)$ is also reversed since the Ikeda map is orientation preserving. There exists the period 2 hyperbolic orbit $H_1(0.5772, 0.6788)$, $(0.3102, -0.7009)$ with transverse intersection of the stable $W^u(H_1)$ and unstable $W^u(H_1)$ manifolds forming the chaotic attractor $A_2 = W^u(H_1)$ (see Fig. 16.5,b). The attractor

A_2 has two connected components derived from components of the unstable manifold $W^u(H_1)$ for points of the orbit H_1. The attractor A_2 can be viewed as a two-periodic attractor since the Ikeda map takes one connected component of A_2 onto the other one. The unstable manifold $W^u(H)$ of the period 2 hyperbolic orbit $H(-0.1364, -0.3495)$, $(0.9931, -0.1676)$ is formed by two separatrices $W^u(H)_1$ and $W^u(H)_2$, which ends at the attractors A_1 and A_2, respectively. Thus, the closure of $W^u(H)$ makes up the attractor $A = A_1 + W^u(H) + A_2$ of the form $A = S + W^u(A_0) + W^u(H) + W^u(H_1)$ (see Fig. 16.5,c).

The stable manifold $W^s(H_0)$ of the hyperbolic fixed point $H_0(1.5062, -2.5002)$ separates the basins of attraction of the attractor A and the sink $S_0(3.1580, 3.2738)$. The unstable manifold $W^u(H_0)$ of H_0 is formed by two separatrices, the left one ends at the attractor A while the right one ends at the sink S_0. The closure of $W^u(H_0)$ generates the global attractor $A_g = A + W^u(H_0) + S_0$ (see Fig. 16.5,d).

16.2.6 $R = 0.8$

The Ikeda map has the inverse saddle A_0 at approximately $(0.4311, 0.2761)$ (see Fig. 16.6,a). Two unstable separatrices $W^u(H)_S$ of the period 2 orbit $H(0.9429, -0.1339)$, $(-0.0296, -0.2155)$ end at the period 2 sink $S(0.0387, -0.0345)$, $(0.8467, -0.0013)$ while two other ones $W^u(H)$ intersect the stable manifolds $W^s(A_0)$ and $W^s(H_1)$ (colored light) of the saddle A_0 and the period 2 hyperbolic orbit $H_1(0.3844, -0.6761)$, $(0.5798, 0.6644)$. The unstable manifolds $W^u(A_0)$ and $W^u(H_1)$ (colored dark) intersect in turn the stable manifold $W^s(H)$, forming the heteroclinic cycle $A_0 \to H_1 \to H \to A_0$ (see Fig. 16.6,a). The closure of unstable manifolds of the cycle generates the attractor A (see Fig. 16.6,b).

The attractor A contains the sink S and, hence, is not a minimal attractor. The basin of attraction $W^s(A)$ of A is bounded by the stable manifold $W^s(H_0)$ of the saddle fixed point $H_0(1.3219, -2.4527)$, the complement to the closure of $W^s(A)$ is the basin of attraction of the focus $S_0(3.0614, 1.6110)$. As above, the left unstable separatrix $W^u(H_0)_l$ of H_0 ends at the attractor A while the right one $W^u(H_0)_r$ ends at the sink S_0. The global attractor A_g is the closure of the unstable manifold $W^u(H_0)$ of the saddle $H_0 : A_g = W^u(H_0) + A + S_0$. We notice that at $R = 0.7$ the unstable manifold $W^u(A_0)$ ends at the sink S, whereas at $R = 0.8$ the sink S is the limit of the unstable separatrix $W^u(H)$, i.e. a bifurcation occurs.

16.2.7 $R = 0.9$

The Ikeda mapping with $R = 0.9$ has a chaotic minimal attractor named the Ikeda attractor. As R increases from $R = 0.8$ to $R = 0.9$, the following bifurcation occurs: the period 2 sink S and the period 2 hyperbolic orbit H disappear.

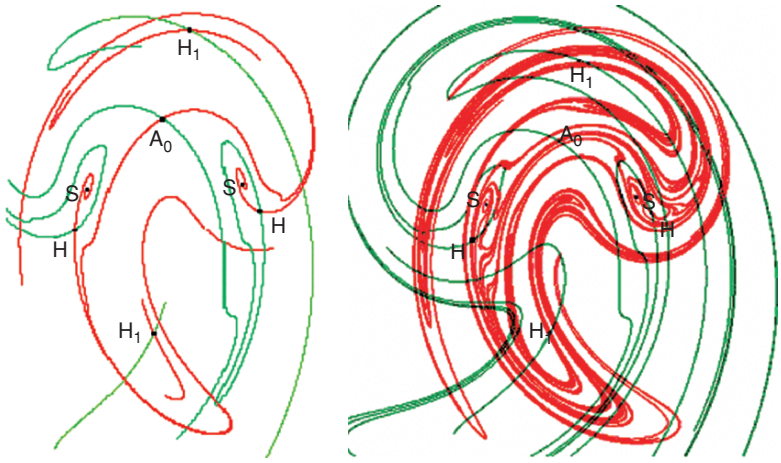

a b

Fig. 16.6. Ikeda map for $R = 0.8$

The attractor A contains the inverse saddle $A_0(0.4819, 0.2645)$ and the period 2 hyperbolic orbit $H_1(0.5964, 0.6394)$, $(0.4497, -0.6453)$. The stable $W^s(A_0)$ and $W^s(H_1)$ and unstable $W^u(A_0)$ and $W^u(H_1)$ manifolds (separatrices) of these saddles intersect and form the heteroclinic cycle $A_0 \to H_1 \to A_0$ (see. Fig. 16.7,a) generating the chaotic attractor A which is the closure of the unstable manifolds $W^u(A_0)$ or $W^u(H_1)$. There exists a pair of the period 3 hyperbolic orbits $P_3(0.8091, 0.7834)$, $(0.9960, -1.0090)$, $(-0.0280, -0.8758)$ and $Q_3(1.3512, -0.0707)$, $(0.6568, -1.1932)$, $(-0.2418, -0.4462)$ (see Fig. 16.7,b). The stable and unstable manifolds of orbits P_3 and Q_3 intersect forming the heteroclinic cycle which also generates the attractor A. The closure of the unstable manifold of any one of the orbits A_0, H_1, P_3 or Q_3 is the attractor A (see Fig. 16.7,c). Outside the attractor A there is the saddle $H_0(1.1987, -2.3769)$ whose left separatrix $W^u(H_0)_l$ ends at the attractor A. The right unstable separatrix $W^u(H_0)_r$ ends at the sink $S_0(3.0027, 3.8945)$ (see Fig. 16.7,d). The stable manifold $W^s(H_0)$ of the saddle H_0 separates the basin of attraction $W^s(A)$ of the attractor A and the basin of attraction $W^s(S_0)$ of the sink S_0. The closure of the unstable manifold $W^u(H_0)$ generates the global attractor $A_g = A + W^u(H_0) + S_0$. The map has no other period 2 and period 3 orbits.

16.2.8 $R = 1.0$

When R goes from 0.9 to $R = 1.0$ the period 1, period 2, and period 3 orbits survive, except that their coordinates vary: when $R = 1.0$ (see Fig. 16.8,a) the inverse saddle A_0 is approximately $(0.5228, 0.2469)$, the period 2 hyperbolic orbit H_1 is approximately $(0.6216, 0.6059)$, $(0.5098, -0.6084)$, and the period 3 hyperbolic orbits P_3 and Q_3 are approximately $(0.7795, 0.7672)$, $(1.0140, -0.9832)$, $(0.0858, -0.8832)$ and $(0.6583, -1.1541)$, $(1.3297, -0.1427)$,

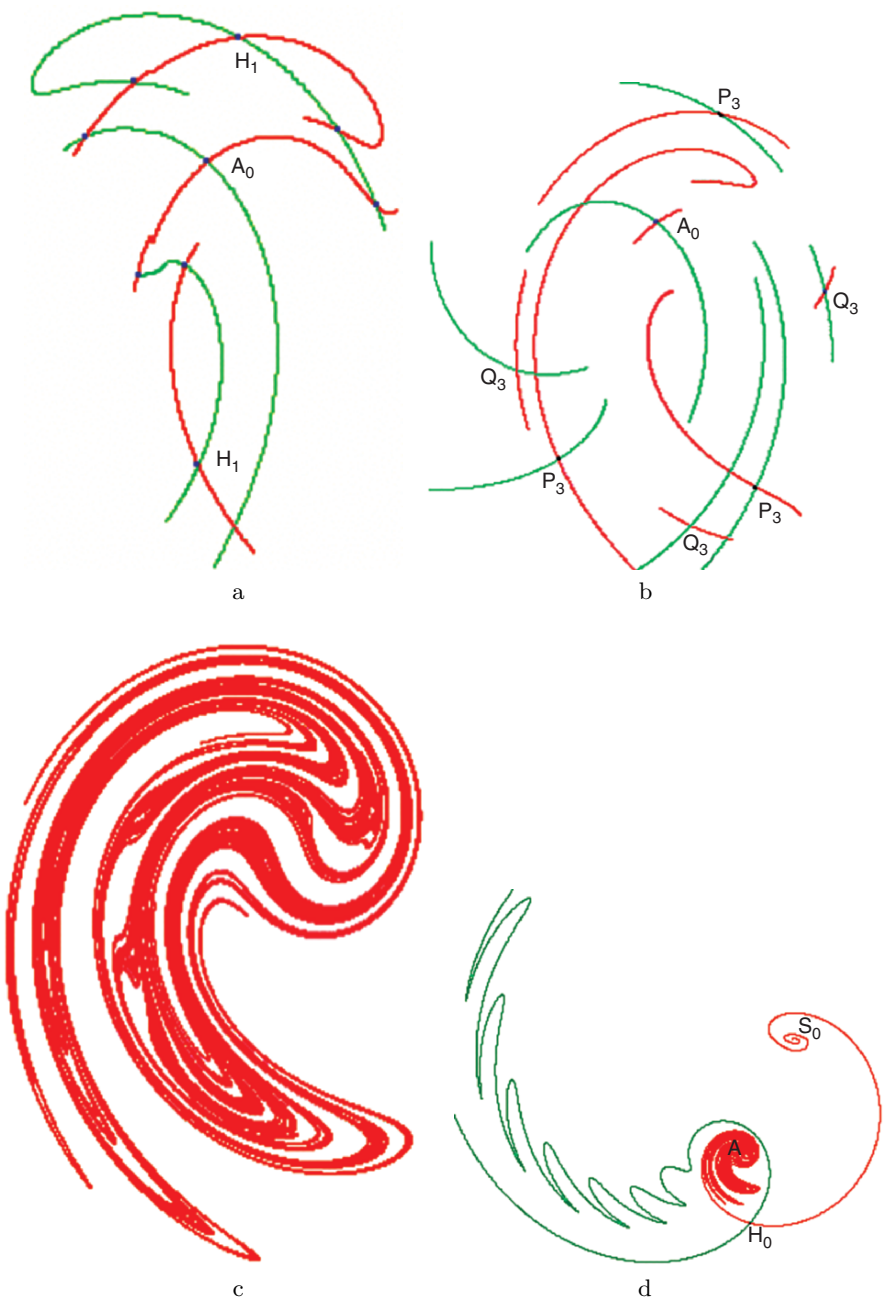

Fig. 16.7. Ikeda map for $R = 0.9$

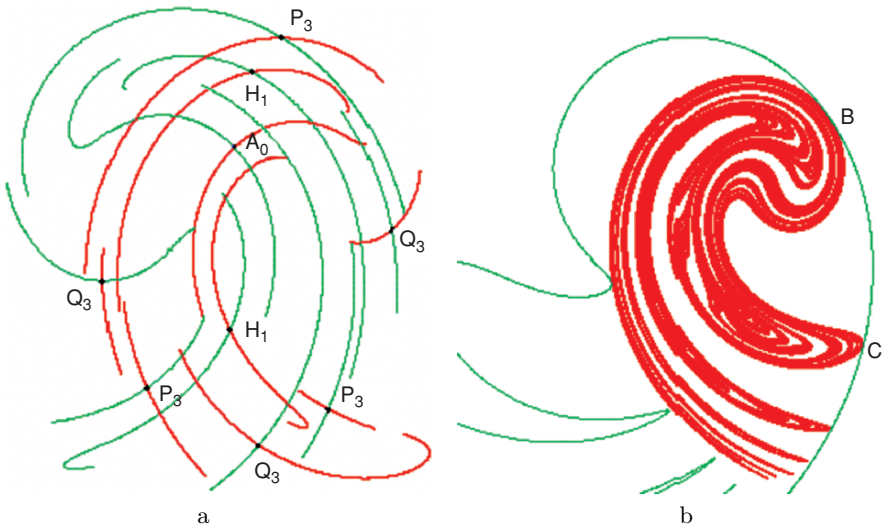

Fig. 16.8. Ikeda map for $R = 1.0$

$(-0.1353, -0.3756)$, respectively. The closure of unstable manifold of any orbit A_0, H_1, P_3 or Q_3 is an attractor A (see Fig. 16.8,b). The basin of attraction of A is bounded by the stable manifold $W^s(H_0)$ of the hyperbolic fixed point $H_0(1.1142, -2.2857)$ which is nearly tangent to A (see Fig. 16.8,b). The enlarged scale phase portraits (Figs. 16.9,c and 16.9,d) show that the distance between A and $W^s(H_0)$ near points B and C is yet positive. The stable manifold $W^s(H_0)$ is a common boundary of the basins of attraction of the attractor A and the sink $S_0(2.9721, 4.1459)$. The stable and unstable manifolds of H_0 are nearly tangent forming a sufficiently fine domain of attraction near points of "nearly tangency". The right separatrix $W^u(H_0)_r$ ends at the sink $S_0(2.9721, 4.1459)$ and the left one $W_u(H_0)_l$ approaches the chaotic attractor A.

16.2.9 $R = 1.1$

The mapping I has the following orbits with periods 1, 2, and 3: the inverse saddle $A_0(0.5837, 0.2232)$, the period 2 orbit $H_2(0.6525, 0.5641)$, $(0.5670, -0.5643)$, and the period 3 orbits $P_3(0.1906, -0.8730)$, $(1.0240, -0.9557)$, $(0.7718, 0.7342)$ and $Q_3(0.6660, -1.0738)$, $(-0.0110, -0.2430)$, $(1.2810, -0.1232)$. The relative positions of these orbits are similar to the case $R = 1.0$. The stable and unstable manifolds of the hyperbolic fixed point $H_0(1.05926, -2.1850)$ intersect transversally generating a homoclinic orbit (Fig. 16.10,a).

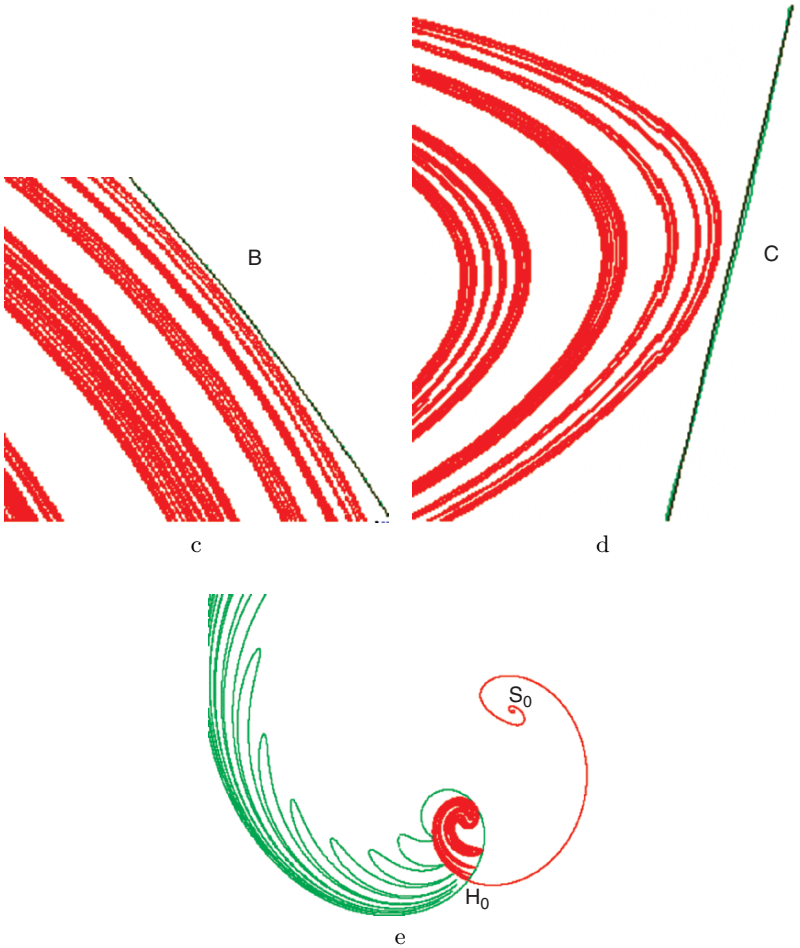

Fig. 16.9. Ikeda map for $R = 1.0$

Fig. 16.10,b displays the manner in which the manifolds $W^s(H_0)$ and $W^u(H_0)$ intersect near H_0. Furthermore, Fig. 16.10,a shows that the stable and unstable manifolds of A_0 and H_0 intersect generating a heteroclinic cycle. Thus, the attractor A fails when R goes from 1.0 to 1.1. The global attractor A_g is the closure of the unstable manifolds of H_0 or A_0. The right unstable separatrix $W^u(H_0)_r$ ends at the focus $S_0(2.9630, 4.3773)$. Moreover, all other unstable manifolds stretching along $W^u(H_0)_r$ approach S_0 as well. The set of chain recurrent points except for S_0 is the closure of points of intersection of $W^s(H_0)$ and $W^u(H_0)$, Fig. 16.11,d displays a neighborhood of the chain recurrent set.

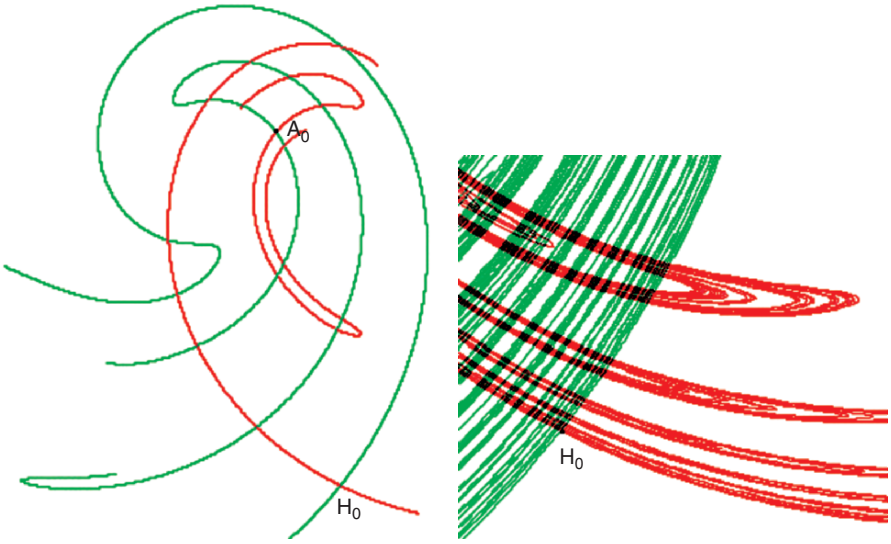

a b

Fig. 16.10. Ikeda map for $R = 1.1$

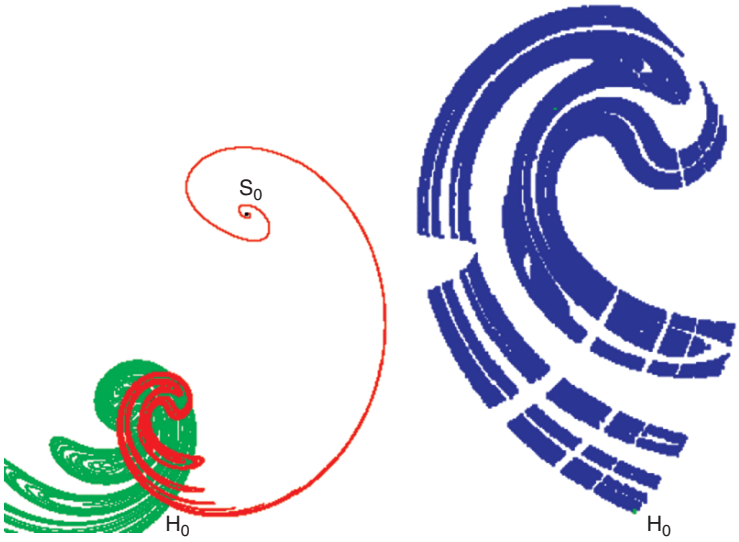

c d

Fig. 16.11. Ikeda map for $R = 1.1$

16.3 Modified Ikeda Mappings

In this section we consider some possible modifications of the Ikeda mapping. With this aim in view, let us rewrite the Ikeda mapping in the form

$$J : (x, y) \mapsto (R + a(x\ \cos\tau - y\ \sin\tau), b(x\ \sin\tau + y\ \cos\tau)), \qquad (16.3)$$

where $\tau = 0.4 - 6/(1+x^2+y^2)$. For the normal Ikeda mapping $a = b = C_2$ and $C_2 \in (0, 1)$, i.e. the mapping is an orientation preserving contraction. Now we will not assume $a = b$, in particular, a and b may be of opposite signs.

16.3.1 Mappings Preserving Orientation

Inverse Attraction: $R = 3$, $a = b = -0.9$

The mapping J has the hyperbolic fixed point $H(1.6030, 0.8268)$ with non-empty intersection of stable and unstable manifolds: $W^s(H) \cap W^u(H)$. The stable and unstable manifolds are nearly tangent at a homoclinic point (Fig. 16.12,a). Since $a = b < 0$, J revises the orientation of $W^s(H)$ and $W^u(H)$ and H is an inverse saddle. There exists the period 2 sink $S(0.0320, 0.3637)$, $(3.3216, -0.0835)$, which is contained in the limit set of $W^u(H)$. The closure of $W^u(H)$ forms the global attractor A_g (Fig. 16.12,b). The global attractor involves the chain recurrent set Q, which contains the orbits H and S and the points of intersection of $W^s(H)$ and $W^u(H)$ (homoclinic points).

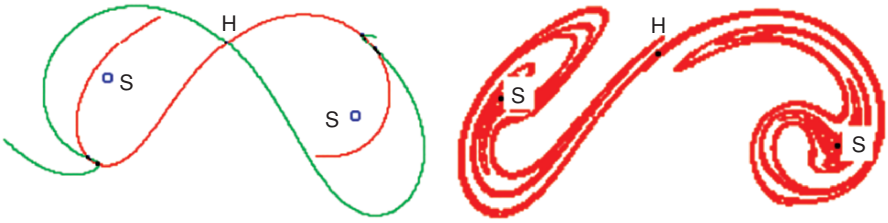

a b

Fig. 16.12. Ikeda map for $R = 3$, $a = b = -0.9$

c d

Fig. 16.13. Ikeda map for $R = 3$, $a = b = -0.9$

A neighborhood of Q obtained by the symbolic dynamics methods is shown in Fig. 16.13,c. A neighborhood of S (colored dark) is a lower bound for a basin of attraction of S. The manifolds $W^s(H)$ and $W^u(H)$ and their intersection points are presented in Fig. 16.13,d. The set of homoclinic points $W^s(H) \cap W^u(H)$ is a lower bound for the chain recurrent set Q.

Hyperbolic Mapping: $R = 1$, $a = 0.9$, $b = 1.2$

There exists hyperbolic fixed point $H(-0.1824, -2.3536)$ with nonempty intersection of the stable and unstable manifolds. The stable and unstable manifolds of H and the point $F(0.0851, 0.9643)$ homoclinic to H are shown in Fig. 16.14,a. Table presents numerical results of successive computation of points H and F.

Step	Fixed point	Homoclinic point
30	$x = -0.18235986$, $y = -2.35361944$	$x = -0.08509742$, $y = 0.96427872$
31	$x = -0.18235987$, $y = -2.35361803$	$x = -0.08144479$, $y = 0.96428413$
32	$x = -0.18235936$, $y = -2.35361106$	$x = -0.08519972$, $y = 0.96428226$

The mapping has the hyperbolic fixed point $H_1(0.5153, 0.2835)$ and the period 2 hyperbolic orbit $P(0.3708, 0.6824)$, $(0.5505, -0.7136)$. The stable and unstable manifolds of H, H_1 and P intersect generating heteroclinic cycles (see Fig. 16.14,b). Fig. 16.14,c shows how the stable and unstable manifolds of P are situated. The set of points homoclinic to H (constructed as an intersection of $W^s(H)$ and $W^u(H)$) is a lower bound of the chain-recurrent set Q and is depicted in Fig. 16.14,d. A neighborhood of Q (an upper bound) obtained by localization using symbolic dynamics methods is displayed in Fig. 16.15,e. The stable manifold $W^s(H)$ of H and stable manifolds of all other orbits from Q start from the source $S(-2.9622, 5.8918)$, see Fig. 16.15,f.

Expansion: $R = 1$, $a = b = 1.2$

The mapping J increases an area by $a^2 = 1.44$ and has a global repeller R_g. This repeller contains the hyperbolic fixed point $H(0.4368, 0.3100)$ which stable and unstable manifolds intersect generating a homoclinic contour. The fixed point H is an inverse saddle, i.e. the map J reverses orientation on $W^s(H)$ and $W^u(H)$. In addition, there exists the 2-periodic orbit $H_1(0.5132, -0.7463)$, $(0.1850, 0.7191)$ whose stable $W^s(H_1)$ and unstable $W^u(H_1)$ manifolds intersect each other and stable $W^s(H)$ and unstable $W^u(H)$ manifolds of H generating a heteroclinic contour (see Fig. 16.16,a). The closure of $W^s(H)$ (or $W^s(H_1)$) forms the repeller R. Fig. 16.16,b presents the repeller R and the manifolds $W^s(H)$ and $W^u(H)$. The set of points (colored dark) of intersection of stable and unstable manifolds of H and H_1 (a lower bound for Q) is depicted in Fig. 16.16,b. Obtained by symbolic dynamics methods, a neighborhood of the chain-recurrent set Q (an upper bound)

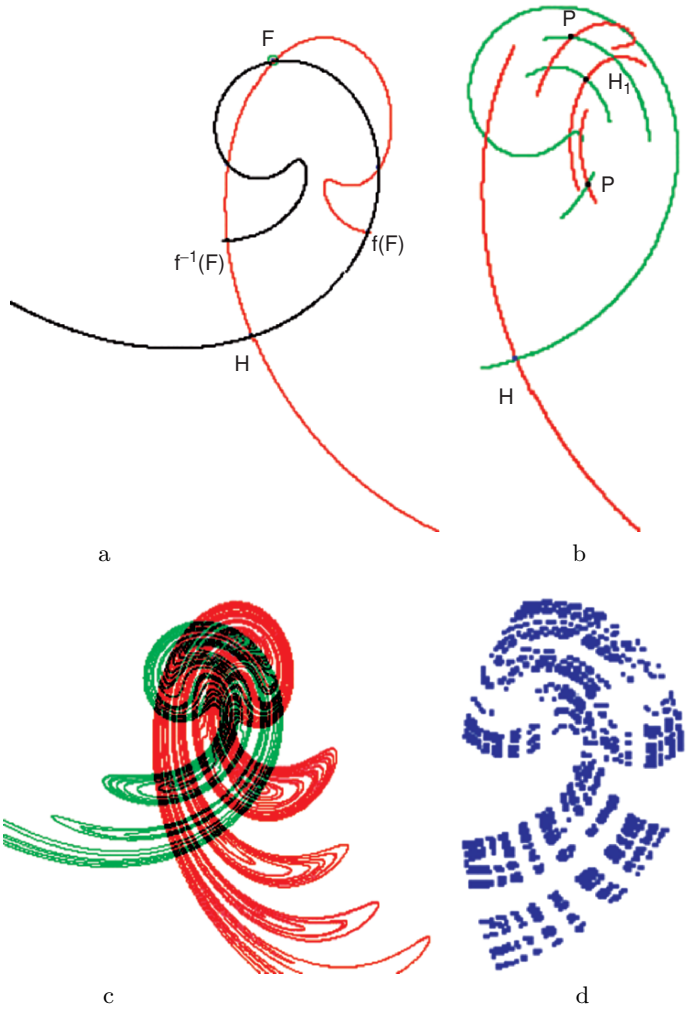

Fig. 16.14. Ikeda map for $R = 1$, $a = 0.9$, $b = 1.2$

containing R is shown in Fig. 16.17,c. It seems likely that $R = Q$. Outside R there exists a hyperbolic fixed point $H_0(-1.2588, -2.5318)$ (see Fig. 16.17,d), the left separatrix of which starts from R and the right one starts from the source $S(-3.7022, 2.3228)$.

16.3.2 Mappings Reversing Orientation

Contraction: $R = 1$, $a = 0.9$, $b = -0.9$

The map J decreases an area and has a global attractor A_g. There exist two hyperbolic fixed points $H_0(0.5726, 0.6602)$ and $H_1(0.5606, -0.5692)$

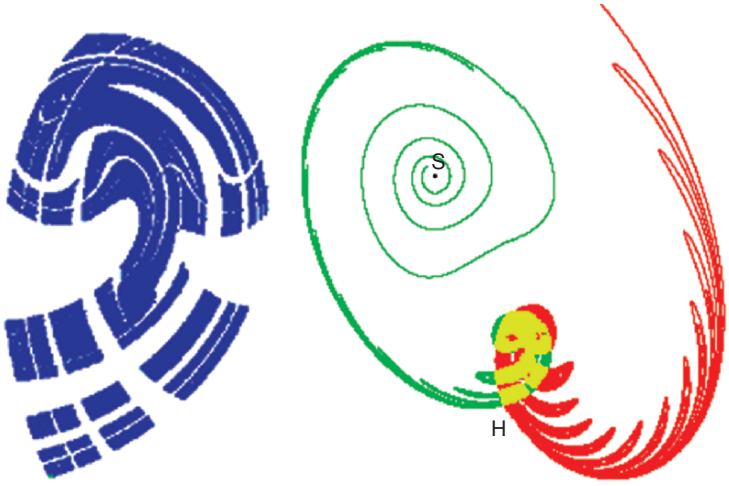

e f

Fig. 16.15. Ikeda map for $R = 1$, $a = 0.9$, $b = 1.2$

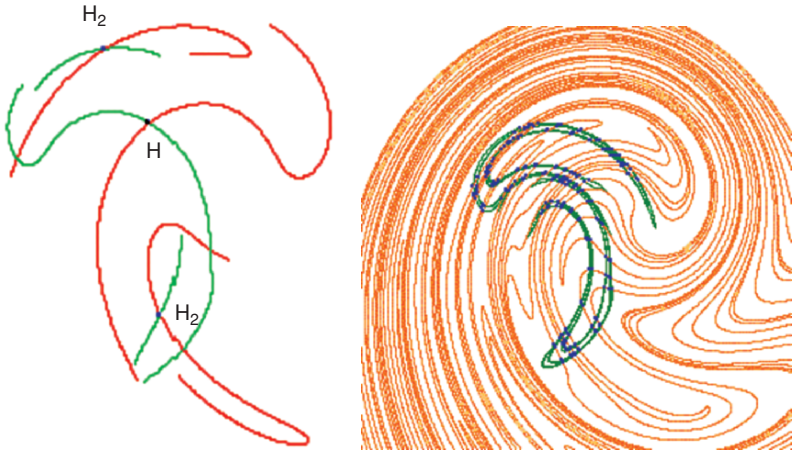

a b

Fig. 16.16. Ikeda map for $R = 1$, $a = b = 1.2$

whose stable and unstable manifolds intersect forming a heteroclinic cycle. In addition, there is a unique 2-periodic hyperbolic orbit $P(0.9391, -0.2036)$, $(0.1539, 0.1791)$ whose stable (unstable) manifold intersects $W^u(H_0)$ and $W^u(H_1)$ ($W^s(H_0)$ and $W^s(H_0)$) forming a heteroclinic cycle (Fig. 16.18,a). Points of intersection of stable and unstable manifolds of these orbits (colored dark in Fig. 16.18,b) yield a lower bound for the chain-recurrent set Q. An upper bound for Q obtained by symbolic dynamics methods is depicted in

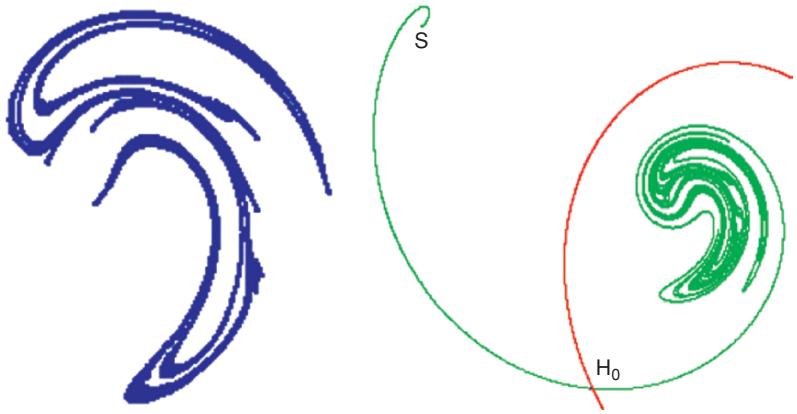

Fig. 16.17. Ikeda map for $R = 1$, $a = b = 1.2$

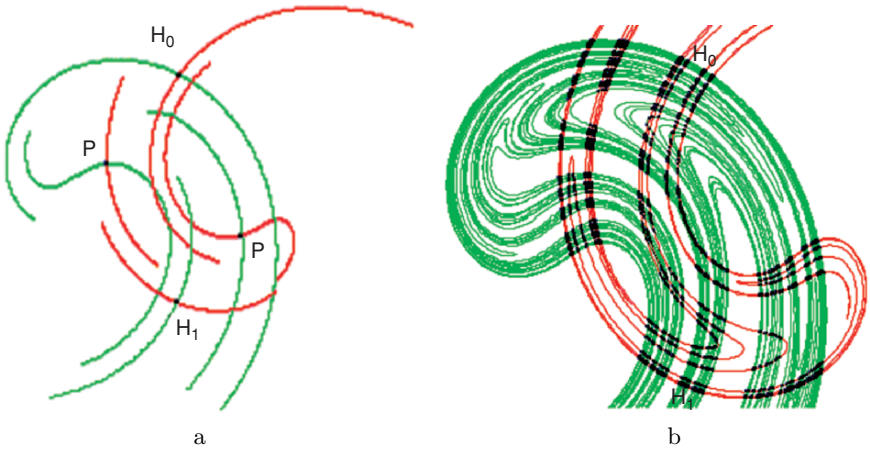

Fig. 16.18. Ikeda map for $R = 1$, $a = 0.9$, $b = -0.9$

Fig. 16.19,c. Near H_0 the manifold $W^s(H_0)$ bounds Q, with the left separatrix $W^u(H_0)_l$ involved in Q and the right one $W^u(H_0)_r$ going to the right (Figs. 16.19,a,b and d). Near H_1 the manifold $W^u(H_1)$ bounds Q, with the right separatrix $W^u(H_1)_r$ involved in Q and the left one $W^u(H_1)_l$ going to infinity (Figs. 16.18,a,b). Stretching along the right separatrix $W^u(H_0)_r$, unstable manifolds start from Q and end at the sink $S(9.7301, -1.5751)$. Stable manifolds start from Q and along the left separatrix $W^s(H_0)_l$ reach infinity in the form of "rabbit ears" (Fig. 16.19,d and Fig. 16.20). The global attractor A_g is the closure of $W^u(H_0)$ (Fig. 16.20).

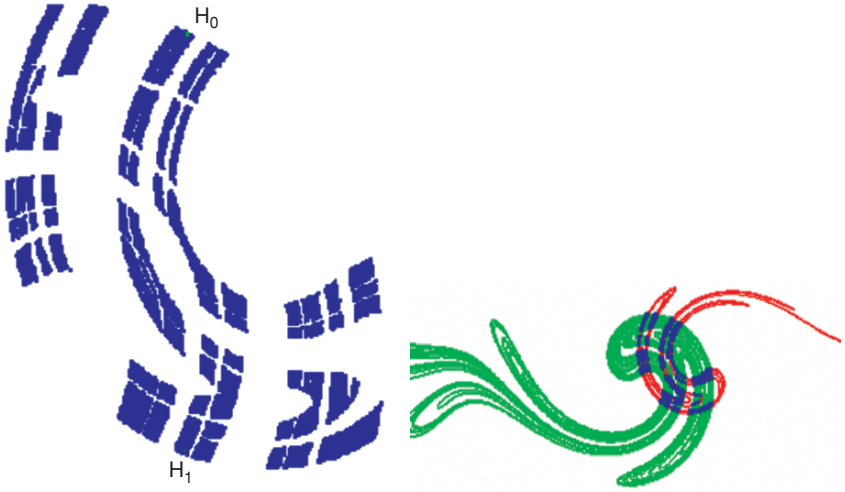

c d

Fig. 16.19. Ikeda map for $R = 1$, $a = 0.9$, $b = -0.9$

Fig. 16.20. Ikeda map for $R = 1$, $a = 0.9$, $b = -0.9$

Contraction: $R = 2$, $a = -0.9$, $b = 0.9$.

The map J decreases an area and the global attractor A_g. There exists the unique hyperbolic fixed point $H(1.3815, -2.4746)$ (Fig. 16.21,a) whose stable and unstable manifolds $W^s(H)$ and $W^u(H)$ intersect (Fig. 16.21,a and b). In addition, there is the unique periodic orbit $P_2(0.2378, -0.7031)$, $(1.9995, 0.6681)$ stable and unstable manifolds of which intersect $W^s(H)$ and $W^u(H)$ forming a heteroclinic cycle (Fig. 16.21,a). The global attractor A_g is a closure of $W^u(H)$ or $W^u(P)$ (Fig. 16.21,b). The set $W^s(H) \cap W^u(H)$ is a lower bound for the chain-recurrent set Q. Fig. 16.21,c presents a neighborhood of Q constructed by symbolic dynamics methods. Since A_g contains all limit points, stable manifolds of orbits from A_g cover the plane R_2. Using symbolic dynamics methods we obtain the 6-period hyperbolic orbit P_6 $(1.0847, -1.0732)$, $(2.7889, -1.1242)$, $(-0.2626, -1.4846)$, $(3.3560, 0.0508)$, $(-1.0124, -0.2235)$, $(1.3964, 0.7116)$. Its Lyapunov exponents are calculated by $\lambda = \frac{1}{6} \cdot \ln|\gamma|$, where by are the eigenvalues of the differential of the Ikeda mapping along the orbit P_6. We obtain: $\gamma_1 = -23.098$, $\gamma_2 = -0.012$ and $\lambda_1 = 0.523$ and $\lambda_2 = -0.734$. The attractor has the 2-periodic orbit P_2 $(0.2385, -0.7024)$, $(1.9989, 0.6691)$. The eigenvalues of the differential

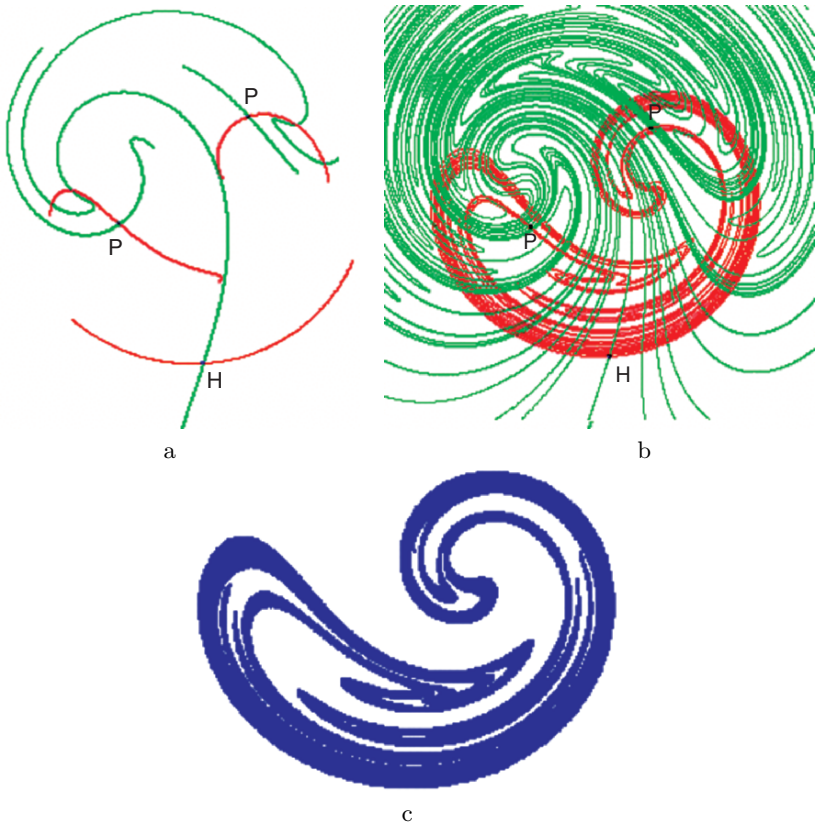

Fig. 16.21. Ikeda map for $R = 2$, $a = -0.9$, $b = 0.9$

along P_2 are $\lambda_1 = -0.134$, $\gamma_2 = -4.888$, and the Lyapunov exponents $\lambda = \frac{1}{2} \cdot \ln|\gamma|$ are $\lambda_1 = -1.004$, $\lambda_2 = 0.793$. There exists the 4-periodic orbit $P_4(-0.6836, -0.6319)$, $(0.7312, -0.9389)$, $(1.6003, 0.72792)$, $(3.0613, -0.1713)$ with the Lyapunov exponents $\lambda_1 = -0.843$, $\lambda_2 = 0.633$.

Hyperbolic Mapping: $R = 1$, $a = -0.9$, $b = 1.2$

The map J has the hyperbolic fixed point $H(-0.0950, 2.1937)$ stable manifold $W^s(H)$ of which can be bijectively projected on the x-axis. The map J reverses orientation on $W^s(H)$. The unstable manifold $W^u(H)$ can be bijectively projected on the y-axis near H, however, the lower part of $W^u(H)$ offers a complicated structure (Fig. 16.22,a). Such a behavior of $W^u(H)$ results from the fact that $W^u(H)$ intersects the stable manifold $W^s(Q_2)$ of the 2-periodic hyperbolic orbit $Q_2(-1.5584, -1.9046)$, $(3.0088, -1.2438)$, which in turn has a homoclinic point of transverse intersection of stable and unstable manifolds

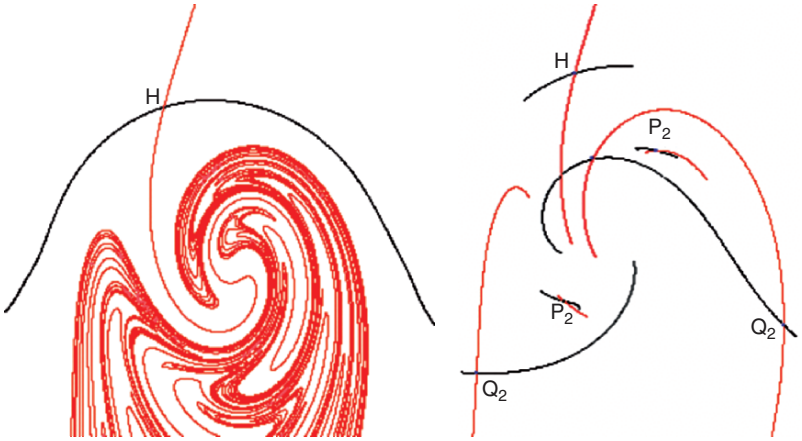

Fig. 16.22. Ikeda map for $R = 1$, $a = -0.9$, $b = 1.2$

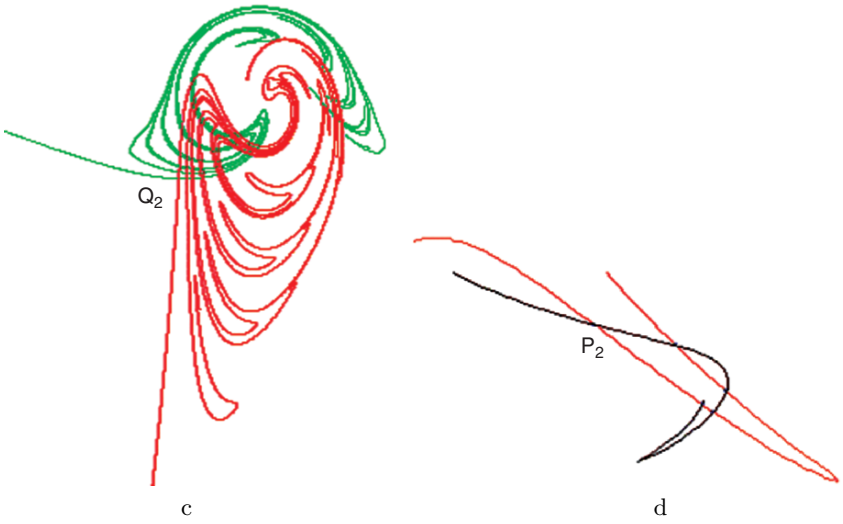

Fig. 16.23. Ikeda map for $R = 1$, $a = -0.9$, $b = 1.2$

$W^u(Q_2)$ and $W^s(Q_2)$ (Fig. 16.22,b). Fig. 16.23,c shows the manner in which $W^u(Q_2)$ and $W^s(Q_2)$ intersect near $Q_2(-1.5584, -1.9046)$. Besides Q_2 there is another 2-periodic hyperbolic orbit $P_2(-0.2554, -0.9207)$, $(1.1152, 1.1362)$ with homoclinic intersection of its stable and unstable manifolds $W^u(P_2)$ and $W^s(P_2)$. Fig. 16.23,d shows the manner in which $W^u(P_2)$ and $W^s(P_2)$ intersect near $P_2(-0.2554, -0.9207)$. Stable and unstable manifolds of orbits Q_2 and P_2 intersect forming a heteroclinic cycle. This leads to the chaotic

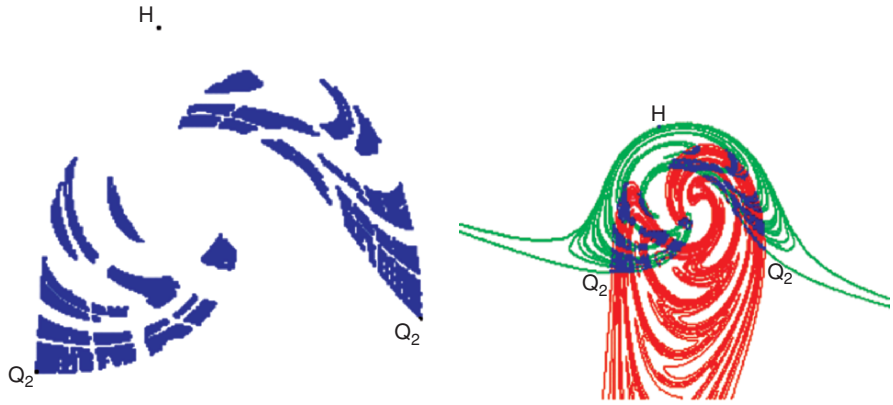

e f

Fig. 16.24. Ikeda map for $R = 1$, $a = -0.9$, $b = 1.2$

chain-recurrent set Q. Fig. 16.24,e depicts a neighborhood (an upper bound) of Q. The set $W^u(Q_2) \cap W^s(Q_2)$ gives a lower bound for Q. Fig. 16.24,f shows the displacement of $W^u(Q_2)$, $W^s(Q_2)$, and their points of intersection. The stable manifold $W^s(H)$ is in the closure of $W^s(Q_2)$. The closure of $W^s(Q_2)$ forms the set looking like a "Napoleon" hat (Fig. 16.24,f).